AGU PUBLICATIONS

JGR

Journal of Geophysical Research: Oceans

RESEARCH ARTICLE

10.1002/2015JC011264

Key Points:
- Lagrangian sampling schemes were used to measure export, production, and grazing processes
- Four satellite algorithms were used to predict export efficiency from in situ plankton measurements
- A food-web based approach performed well, while also realistically predicting grazing rates

Supporting Information:
- Supporting Information S1
- Table S1

Correspondence to:
M. R. Stukel,
mstukel@fsu.edu

Citation:
Stukel, M. R., M. Kahru, C. R. Benitez-Nelson, M. Décima, R. Goericke, M. R. Landry, and M. D. Ohman (2015), Using Lagrangian-based process studies to test satellite algorithms of vertical carbon flux in the eastern North Pacific Ocean, *J. Geophys. Res. Oceans*, *120*, 7208–7222, doi:10.1002/2015JC011264.

Received 25 AUG 2015
Accepted 7 OCT 2015
Accepted article online 19 OCT 2015
Published online 6 NOV 2015

Using Lagrangian-based process studies to test satellite algorithms of vertical carbon flux in the eastern North Pacific Ocean

M. R. Stukel[1], M. Kahru[2], C. R. Benitez-Nelson[3], M. Décima[4], R. Goericke[2], M. R. Landry[2], and M. D. Ohman[2]

[1]Department of Earth, Ocean, and Atmospheric Science, Florida State University, Tallahassee, Florida, USA, [2]Scripps Institution of Oceanography, University of California at San Diego, La Jolla, California, USA, [3]Marine Science Program and Department of Earth and Ocean Sciences, University of South Carolina, Columbia, South Carolina, USA, [4]National Institute of Water and Atmospheric Research, Wellington, New Zealand

Abstract The biological carbon pump is responsible for the transport of ~5–20 Pg C yr^{-1} from the surface into the deep ocean but its variability is poorly understood due to an incomplete mechanistic understanding of the complex underlying planktonic processes. In fact, algorithms designed to estimate carbon export from satellite products incorporate fundamentally different assumptions about the relationships between plankton biomass, productivity, and export efficiency. To test the alternate formulations of export efficiency in remote-sensing algorithms formulated by Dunne et al. (2005), Laws et al. (2011), Henson et al. (2011), and Siegel et al. (2014), we have compiled in situ measurements (temperature, chlorophyll, primary production, phytoplankton biomass and size structure, grazing rates, net chlorophyll change, and carbon export) made during Lagrangian process studies on seven cruises in the California Current Ecosystem and Costa Rica Dome. A food-web based approach formulated by Siegel et al. (2014) performs as well or better than other empirical formulations, while simultaneously providing reasonable estimates of protozoan and mesozooplankton grazing rates. By tuning the Siegel et al. (2014) algorithm to match in situ grazing rates more accurately, we also obtain better in situ carbon export measurements. Adequate representations of food-web relationships and grazing dynamics are therefore crucial to improving the accuracy of export predictions made from satellite–derived products. Nevertheless, considerable unexplained variance in export remains and must be explored before we can reliably use remote sensing products to assess the impact of climate change on biologically mediated carbon sequestration.

1. Introduction

The ocean contains approximately 50 times more inorganic carbon than the atmosphere, but its ability to absorb atmospheric CO_2 is restricted by the rate of transport of carbon from the surface ocean (which communicates directly with the atmosphere) to the deep ocean. The ocean's ability to sequester anthropogenic CO_2 for periods longer than a season is dependent on two types of processes that transport inorganic carbon to the ocean interior: the solubility pump and the biological carbon pump (BCP) [*Raven and Falkowski*, 1999]. The solubility pump is driven by the increased solubility of CO_2 in cold, dense water and is hence dependent on physical and chemical processes that are mechanistically understood. The BCP refers to the sum of several different biological processes (sinking of particulate carbon, active vertical migrations, and advective and diffusive transport of particulate and dissolved organic carbon to depth) mediated by plankton and other marine organisms that transport organic carbon to depth [*Ducklow et al.*, 2001]. The BCP remains poorly constrained. Of particular importance to the BCP is the gravitational flux of sinking particles (hereafter simply referred to as carbon export) derived ultimately from photosynthesis, but with rates that are dependent on complex food-web transformations [*Turner*, 2015]. This portion of the biological pump has been estimated to sequester between 5 and 21 Pg C yr^{-1} in the deep ocean [*Laws et al.*, 2000; *Boyd and Trull*, 2007; *Henson et al.*, 2011; *Siegel et al.*, 2014; *Henson et al.*, 2015]. However, its magnitude, variability, and especially its potential response to climatic forcing remain difficult to quantify [*Passow and Carlson*, 2012].

Due to the variety of issues associated with autonomous in situ measurements of carbon export (though see recent advances outlined in *Bishop* [2009] and *McDonnell et al.* [2015]), and the expense of

oceanographic expeditions, accurate remote sensing of carbon export has been a goal of marine biogeochemists for decades. Traditional approaches have started with estimates of vertically integrated primary production (PP) derived from near-sea surface chlorophyll (SSChl), sea surface temperature (SST) and surface irradiance [*Behrenfeld and Falkowski*, 1997; *Westberry et al*., 2008], which are then multiplied by an export ratio (*e*-ratio = carbon export/PP). Export ratio formulations typically stem from mechanistic frameworks that quantify particular hypotheses about the processes regulating carbon export (e.g., the temperature dependency of remineralization rates [*Henson et al*., 2011] or the dominant role of large phytoplankton and zooplankton in vertical export [*Laws et al*., 2000]). The underlying functional relationships suggested by these mechanistic frameworks are then combined with satellite measurable parameters (i.e., SST, SSChl, or primary production) and empirically fit to match in situ measurements of carbon export. Export ratio formulations have been fit to relationships with SST and PP [*Laws et al*., 2000; *Laws*, 2004; *Laws et al*., 2011], SST and SSChl [*Dunne et al*., 2005, 2007], and SST alone [*Henson et al*., 2011]. While these algorithms are capable of predicting inter-regional variability in carbon export, they often struggle to predict intra-regional variations [*Dunne et al*., 2005], thus limiting their use for assessing temporal variations of carbon export.

The model formulation by *Siegel et al*. [2014] uses a different approach; it grounds *e*-ratio calculations in an explicit depiction of the marine food web. This ecosystem model is built on the assumption that vertical carbon flux is dominated by the sinking of ungrazed microphytoplankton (cells >20 μm) and the fecal pellets of mesozooplankton. While such a formulation is common in NPZD-type models, its applicability to satellite estimation of carbon export is only possible due to two novel aspects of the *Siegel et al*. [2014] approach. The first involves time–series determinations of net rates of change of phytoplankton biomass, which are then combined with phytoplankton production rates in a mass balance equation to estimate grazing rates. The second is the use of the *Kostadinov et al*. [2009, 2010] algorithm to estimate the particle size spectrum from particle backscattering spectra as derived from the SeaWiFS satellite sensor. With these combined approaches, *Siegel et al*. [2014] were able to estimate carbon export (the sum of sinking algal aggregates and fecal pellets) from satellites by first estimating microphytoplankton production and mesozooplankton and protozoan grazing rates. The *Siegel et al*. [2014] model is thus unique among commonly used satellite algorithms in that none of its parameters are empirically fit and that crucial intermediary results can also be tested against in situ measurements. Evaluation of the accuracy of grazing prediction can thus determine whether the algorithm is appropriately encoding a mechanistic understanding of the system or is simply getting approximately correct *e*-ratios due to other correlations between its input parameters and export (e.g., between size-spectrum and *e*-ratio).

While many of the empirical algorithms can (and have been) tested by direct comparison of satellite estimates of export to in situ carbon export measurements, this validation approach suffers from the difficulty of disentangling errors associated with inaccuracies of remote sensing products (e.g., primary productivity, SSChl, and SST) and errors associated with the model used to estimate the *e*-ratio. An alternative approach is to use only in situ measurements to estimate the magnitude of BCP and to compare these estimates to carbon export rates measured by sediment traps [*Knauer et al*., 1979] or the ^{238}U-^{234}Th disequilibrium method [*Buesseler et al*., 1992]. While it is fairly simple to compile the necessary measurements for estimating export for some of the empirical models (e.g., the *Henson et al*. [2011] algorithm requires only PP and SST) fewer data sets are available that can be used to assess the accuracy of the *Siegel et al*. [2014] algorithm, since in addition to PP it also requires an estimate of the ratio of microphytoplankton biomass to total phytoplankton biomass and the net rate of change of phytoplankton in the water column. Testing this algorithm thus requires a Lagrangian approach to measure in situ rates of net phytoplankton growth. Additionally, contemporaneous measurements of mesozooplankton and protozoan grazing rates are important for validating the intermediary results of the algorithm. To this end, we have compiled results from Lagrangian process studies conducted by the California Current Ecosystem (CCE) Long Term Ecological Research (LTER) and Costa Rica Dome (CRD) FLUx and Zinc Experiments (FLUZiE) to compare the efficacies of the *Dunne et al*. [2005], *Laws et al*. [2011], *Henson et al*. [2011], and *Siegel et al*. [2014] satellite algorithms.

This manuscript is not, however, intended to be a definitive comparison of competing satellite algorithms. Rather, we view it as a starting point in a process of using multiple, complementary food-web measurements to mechanistically assess the potentially problematic assumptions or parameterizations in current satellite algorithms so that they can be improved upon or superseded by more accurate models.

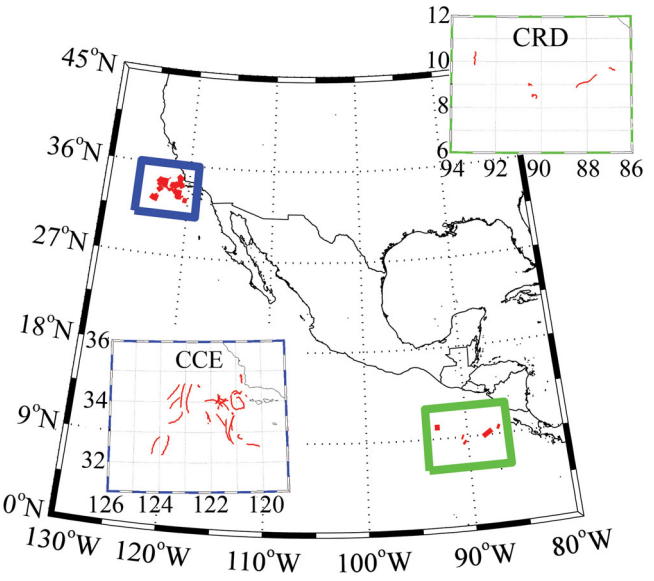

Figure 1. Lagrangian cycle locations. CCE drifter tracks (blue box, lower left). CRD drifter tracks (green box, upper right).

2. In Situ Methods and Data Sets

2.1. Study Design and Data Sets

Data sets were derived from Lagrangian process studies (herein referred to as experimental cycles) of 2–5 day durations conducted in the California Current Ecosystem (CCE) or the Costa Rica Dome (CRD) during which shallow-drifting sediment traps or ^{238}U-^{234}Th methods (or more typically both) were used to measure gravitational carbon export. These two methods, though not without their individual flaws [*Baker et al*., 1988; *Savoye et al*., 2006; *Buesseler et al*., 2007], are currently the most widely used methods for quantifying carbon export out of the euphotic zone. Although neutrally buoyant sediment traps (NBSTs) may be more accurate, they are both expensive and not ideally suited to experiments involving Lagrangian tracking of surface layers because they travel autonomously in subsurface layers while not in communication with surface ships. The Lagrangian process studies in the present data set involved satellite-tracked surface-tethered drifters with a 3 m × 1 m holey-sock drogue centered at 15 m depth, and with either experimental incubation bottles or VERTEX-style sediment traps attached below [*Landry et al*., 2009; *Stukel et al*., 2013a]. For the CCE cruises, selection of water parcels was preceded by site surveys using a free-fall Moving Vessel Profiler [*Ohman et al*., 2012]. Quasi-lagrangian tracking of water parcels during these studies allowed simultaneous measurement of carbon export, food web processes (primary production, protozoan grazing, mesozooplankton grazing, size-spectra of phytoplankton community), and net changes of in situ water column standing stocks of chlorophyll *a* (Chl *a*). Unlike the other models to be compared, this full suite of measurements is necessary for testing the *Siegel et al*. [2014] satellite algorithm.

Data sets for this study were derived from 7 cruises (6 of which occurred in the southern California Current Ecosystem (CCE), and the other in the Costa Rica Dome (CRD), for a total of 32 Lagrangian experiments, Figure 1 and Table 1). During CCE-P0605 in May 2006, 5 distinct regions were investigated, spanning an onshore-offshore gradient (near CalCOFI line 80) from near the Point Conception upwelling center across the California Current proper (CC) and into the edge of the oligotrophic subtropical North Pacific gyre [*Landry et al*., 2009; *Stukel et al*., 2011, 2012]. CCE-P0704 occurred during April 2007 and sampled both the CC and a high biomass region near Point Conception, where high mesozooplankton top-down grazing pressure drove a decrease in phytoplankton biomass [*Landry et al*., 2009; *Stukel et al*., 2012, 2013a]. CCE-P0810 occurred during October 2008, when unexpectedly high winds from the north likely drove fall upwelling near Point Conception. An onshore-offshore gradient along CalCOFI line 80 was sampled in addition to regions south and north of a front separating recently upwelled water from warmer water of CC and/or subtropical origin [*Landry et al*., 2012; *Ohman et al*., 2012; *Taylor et al*., 2012; *Stukel et al*., 2013a]. CCE-P0904 in April 2009 again sampled water parcels in the region offshore of Point Conception (M. Stukel, unpublished data, 2015). CCE-P1106 sampled water parcels within a gradient region between anticyclonic and cyclonic eddies south and west of the California Channel Islands [*Brzezinski et al*., 2015; *Krause et al*., 2015; M. Stukel, unpublished data, 2015]. CCE-P1208 sampled water parcels within and to either side of a frontal feature originating north of CalCOFI line 80 [*Bednarsek and Ohman*, 2015; M. Stukel, unpublished data, 2015]. The CRD FLUZiE cruise sampled waters influenced by the Costa Rica upwelling Dome during June 2010 (a mild El Niño) when SSChl was slightly depressed relative to climatological means [*Stukel et al*., 2013b; M. R. Landry et al., Plankton dynamics and biogeochemical fluxes in the Costa Rica Dome: Introduction to the CRD Flux and Zinc Experiments, submitted to *Journal of Plankton Research*, 2015]. Data sets used for this study (see supporting information Table S1) are either previously published and/or available from the CCE Long-Term Ecological

Table 1. Cruise Overviews[a]

Cruise	Month	Study Site	SST (°C)	SSChl (μg L^{-1})
CCE-P0605	May	Coastal-offshore CCE	12.2–16.4	0.09–5.94
CCE-P0704	Apr.	Coastal-offshore CCE	12.2–14.2	0.22–1.35
CCE-P0810	Oct.	Coastal-offshore CCE	15.0–17.2	0.20–1.47
CCE-P0904	Apr.	Front ~100 km from Point Conception	12.5–13.8	0.23–0.60
CCE-P1106	June	Gradient region, 80–130 km from shore	14.3–16.0	0.12–3.71
CCE-P1208	Aug.	Front between eddies, 160–240 km from shore	14.8–17.0	0.10–2.59
CRD	July	Costa Rica upwelling Dome	27.5–28.5	0.19–0.26

[a]Month, brief description of the study location, and ranges of sea surface temperature and sea surface Chl *a* are given for the seven cruises used in this manuscript.

Research Datazoo website (http://oceaninformatics.ucsd.edu/datazoo/data/ccelter/datasets) or the Biological and Chemical Oceanography Data Management Office (http://www.bco-dmo.org/deployment/58834). Due to the vagaries of cruise plans and unexpected issues at sea, however, not all experimental cycles included all measurements.

2.2. Carbon Export Measurements

Vertical carbon export driven by the gravitational flux of sinking particles was measured by two methods: sediment traps and ^{238}U-^{234}Th disequilibrium. VERTEX-style particle interceptor traps [*Knauer et al*., 1979] with an aspect ratio of 8:1 (height:diameter), inner diameter of 7 cm and a baffle constructed of 14 smaller tubes (similar 8:1 aspect ratio and beveled to a sharp edge on top) were deployed at the beginning and recovered at the end of all Lagrangian experiments (2–5 day cycles), with the exception of CCE-P0605 when only ^{234}Th was measured. Sediment traps were deployed with 2 L of a saltwater brine solution preserved with 4% Formalin. Following recovery, contents of the trap tubes were subsampled with a rotary splitter, sorted with a dissecting microscope to removing swimming mesozooplankton, and filtered through pre-combusted GF/F filters (for organic C/N measurements) or quartz filters (for C:^{234}Th ratios). Carbon contents of the filters (following acidification) were determined at the Scripps Institution of Oceanography Analytical Facility. For CCE cruises, sediment traps were always deployed at a depth of 100 m and (with the exclusion of CCE-P0704), when the euphotic zone was estimated to be shallower than 80 m, an additional trap crosspiece was placed at a depth slightly below the expected euphotic zone (50–70 m). For the CRD FluZiE cruise one crosspiece was placed at a depth of 90 or 100 m, and a second crosspiece was deployed at 150 m (for detailed methods, see *Stukel et al*. [2013a, 2013b]).

For water column ^{234}Th sampling, 8–12 depths were sampled per profile from Niskin bottles on a CTD rosette (typically two profiles per cycle, though occasionally one or three), and ^{234}Th concentrations were determined using standard small-volume techniques [*Pike et al*., 2005]. Briefly, 4 L samples were acidified and spiked with ^{230}Th tracer, and allowed to sit for 4–9 h. Samples were then adjusted back to a pH ~9 and $KMnO_4$ and $MnCl_2$ were added, following which coprecipitation of Th isotopes with manganese oxide occurred for >8 h. Samples were then filtered onto quartz filters that were counted either at sea (CCE-P1208) or at the University of South Carolina immediately following the other cruises on a RISO GM beta multicounter. Samples were background counted >6 half-lives later. Samples were then dissolved and ^{229}Th was added as a yield monitor. Filtration yield (mean = 86% ± 12%, median = 89%) was determined by mass spectroscopy analysis of the $^{229:230}$Th ratio at the Woods Hole Oceanographic Institution Analytical Facility. ^{238}U-^{234}Th deficiencies were determined from linear relationships of ^{238}U with salinity (*Chen et al*. [1986] was used for published results from CCE-P0605, CCE-P0704, and CCE-P0810; *Owens et al*. [2011] was used for CRD and previously unpublished data sets, though differences between relationships were within measurement uncertainty). The deficiencies were converted to ^{234}Th export using a trapezoidal vertical integration of ^{238}U-^{234}Th activity differences to the depth of the shallowest trap depth (typically slightly deeper than the euphotic zone) and then assuming a steady state model [*Savoye et al*., 2006]. Two nearshore cycles that included very recently upwelled water were not considered to be in steady state with respect to ^{234}Th and were excluded from the data set (CCE-P0605 Cycles 1 and 3). All profiles for a given cycle were averaged to determine ^{234}Th export for the cycle. ^{234}Th export was converted to C export by multiplying by C:^{234}Th ratios determined by large (typically >53 μm) particles collected by situ pumps (CCE-P0605), an average of in situ pumps and sediment trap-collected particles (CCE-P0704 and CCE-P0810), or sediment trap-collected particles (CCE-P0904, CCE-P1106, CCE-P1208 and CRD FLUZiE). A total of 621 water column

^{234}Th measurements and 27 sediment trap deployments were used for this study. For detailed methods, see *Stukel et al*. [2011, 2013a, 2015].

Most satellite algorithms are designed explicitly to measure export at the base of the euphotic zone (EZ). Although our export measurements were typically made within ~30 m of the EZ, we wanted to ensure that slight differences between EZ depth and export measurement depth horizon did not bias our results. Hence, we normalized our sediment trap and ^{234}Th-derived carbon export measurements to the depth at which photosynthetically active radiation (PAR) reached 1% of surface PAR. These EZ-normalized values ($Export_{EZ,ST}$ and $Export_{EZ,Th}$) were computed by assuming that export declined with depth as a function of the form;

$$Export(depth = EZ + d) = Export(depth = EZ) \times e^{-\gamma d} \quad (1)$$

To determine the remineralization constant (γ), we used cycles (18 total, 13 from CCE, 5 from CRD) for which we had sediment trap deployments at two depths beneath the euphotic zone. Since the distributions of γ values from CCE and CRD were found to be different based on a Kolmogorov-Smirnov test, we computed separate geometric mean γ values for CCE (0.0063 m^{-1}) and CRD (0.0024 m^{-1}). We then used the shallowest sediment trap (to calculate $Export_{EZ,ST}$) or ^{234}Th-derived (to calculate $Export_{EZ,Th}$) estimate of export and equation (1) to calculate export at the base of the euphotic zone. Since our export measurements were usually only slightly deeper than the EZ, the exact functional form of equation (1) used to compute remineralization as a function of depth had little impact on our results (median correction factor was +15%).

2.3. Food-Web Measurements

To compare the *Siegel et al*. [2014] satellite algorithm results with in situ data, we made several rate measurements of different processes in the plankton food web (in addition to the standard Chl *a* measured by acidification [*Strickland and Parsons*, 1972] and temperature measured by CTD). We measured the net rate of change of in situ euphotic zone chlorophyll by taking the natural log of vertically integrated Chl *a* on succeeding days at the location of our experimental array drifter $\Delta Chl = \ln(Chl_{day=i+1}/Chl_{day=i})$. We measured protozoan grazing rates daily at 8 depths using a modified two-point dilution method [*Landry et al*., 1984, 2009; *Selph et al*., 2015] with samples incubated in situ on our experimental array to ensure accurate light and temperature conditions. Samples were analyzed for bulk Chl *a*, providing both specific growth rates of and grazing rates on the phytoplankton community. Specific growth and grazing rates (μ and m_{micro}, respectively), were then multiplied by initial Chl *a* concentration, vertically integrated, and divided by vertically integrated Chl *a* to determine vertically integrated μ and m_{micro}. On the same experimental arrays, we measured PP at 6–8 depths by the $H^{14}CO_3^-$ uptake method. We determined mesozooplankton grazing rates (m_{meso}) from the pigment contents of mesozooplankton captured in oblique bongo or ring net tows through the upper 150–200 m of the water column [*Landry et al*., 2009; *Décima et al*., 2015; M. D. Ohman, unpublished data, 2008]. Pigment contents were converted to bulk grazing rates by multiplying by either a temperature-specific gut turnover time for CCE samples or a gut turnover time representative of mesozooplankton in tropical waters for CRD samples [*Dam and Peterson*, 1988; *Zhang et al*., 1995]. Bulk grazing rates were then divided by vertically integrated Chl to calculate m_{meso}. We determined the fraction of phytoplankton biomass composed of microplankton using two different methods. The first was epifluorescence microscopy of DAPI and proflavin stained cells identified as autotrophs by their red autofluorescence under blue excitation light (for further details, see *Taylor et al*. [2012] and *Taylor et al*. [2015]). Fractional microphytoplankton biomass was calculated as the vertically integrated biomass of autotroph cells with longest linear dimension >20 μm divided by the vertically integrated biomass of all autotroph cells. We also determined the fraction of microphytoplankton biomass as the ratio of Chl *a* retained on a 20 μm polycarbonate filter to the ratio of Chl *a* retained on a GF/F filter from paired samples taken in the surface mixed layer. In cycles where these two measurements were both made (14 cycles) the microscopy estimate was typically higher (mean of 0.39 ± st. dev. of 0.21) than the size-fractionated Chl estimate (0.23 ± 0.25), although the two measurements were well correlated ($R^2 = 0.54$, $p < 0.01$) (CCE-CalCOFI Methods Manual, http://cce.lternet.edu/data/methods-manual).

2.4. Model Computations

Since our goal was to determine the efficacy of satellite algorithms for determining sinking carbon export efficiency (the *e*-ratio), rather than to evaluate the underlying satellite products from which the *e*-ratio estimates were derived (e.g., SST, SSChl, PP), all satellite algorithms were evaluated from properties measured in situ. Since most satellite algorithms were designed to estimate export at the base of the EZ and some of

our measurements (e.g., mesozooplankton grazing) were only made as EZ vertically integrated rates, we chose to vertically integrate all water column rate and standing stock measurements except when models made explicit reference to sea surface values (e.g., SSChl in *Dunne et al.* [2005]). Following *Dunne et al.* [2005, hereinafter *Dunne* 2005; 2007] we computed:

$$E_{EZ,Dunne} = {}^{14}CPP \times \max(0.04, \min(0.72, -0.0081 \times SST + 0.0806 \times \ln(SSChl) + 0.426) \quad (2)$$

where ^{14}CPP is the vertically integrated $H^{14}CO_3^-$ primary productivity measurement and SST and SSChl are sea surface temperature and Chl *a*, respectively (max and min statements are designed to set limits of 0.04 and 0.72 on the *e*-ratio, following *Dunne*2005). Following *Laws et al.* [2011; hereinafter *Laws*2011], we computed:

$$E_{EZ,Laws2011} = {}^{14}CPP \times 0.04756\left(0.78 - \frac{0.43 \times SST}{30}\right)\left({}^{14}CPP\right)^{0.307} \quad (3)$$

Following Henson et al. [2011; hereinafter *Henson* 2011], which was officially defined as estimating export at the 100 m depth horizon, we computed:

$$E_{100,Henson2011} = {}^{14}CPP \times 0.23 \times e^{-0.08 \times SST} \quad (4)$$

Following *Siegel et al.* [2014; hereinafter *Siegel*2014], we computed:

$$E_{EZ,Siegel2014} = AlgEZ + FecEZ \quad (5)$$

where AlgEZ is the total vertical flux of sinking algal cells and aggregates and FecEZ is the total vertical flux of sinking fecal material released from zooplankton grazers.

$$AlgEZ = f_{Alg} \times NPP_M \quad (6)$$

where f_{Alg} is the fraction of microphytoplankton production that sinks out of the base of the EZ (assumed by *Siegel*2014 to be 0.1) and NPP_M is the production of microphytoplankton, which we compute as the product of ^{14}CPP and the ratio of $>$20 μm phytoplankton to total phytoplankton (calculated from either vertically integrated microscopically derived phytoplankton biomass or mixed layer size-fractionated Chl *a*).

$$FecEZ = f_{FecM} G_M + f_{FecS} G_S \quad (7)$$

where f_{FecM} and f_{FecS} are the fractions of grazing on microphytoplankton and smaller ($<$20 μm) phytoplankton, respectively, that contribute to fecal matter export from the EZ (assumed by *Siegel2014* to be 0.3 and 0.1, respectively). G_M and G_S are the grazing rates on microphytoplankton and small phytoplankton and are derived from phytoplankton mass balance budgets:

$$G_M = NPP_M - \frac{\partial P_M}{\partial t} - m_{ph} P_M - AlgEZ \quad (8)$$

$$G_S = NPP_S - \frac{\partial P_S}{\partial t} - m_{ph} P_S \quad (9)$$

where NPP_s is the primary productivity of small phytoplankton (equal to ^{14}CPP minus NPP_M). $\partial P_M/\partial t$ and $\partial P_S/\partial t$ are the rates of change of microphytoplankton and smaller phytoplankton (respectively) with time (equal to the specific net rate of change of vertically integrated Chl *a* in the EZ multiplied by the ratio of microphytoplankton to total phytoplankton or the ratio of small phytoplankton to total phytoplankton). m_{ph} is the nongrazer related specific mortality of phytoplankton (assumed by *Siegel*2014 to be 0.1 d^{-1}). P_M and P_S are the vertically integrated biomasses of microphytoplankton and smaller phytoplankton (measured directly by microscopy on CCE-P0605, CCE-P0704, CCE-P0810, and CRD and estimated as the product of vertically integrated Chl *a*, a C:Chl ratio (determined from CCE samples) and the ratio of large:-total or small:total phytoplankton determined from size-fractionated Chl *a* samples for other cycles). Note that equations (8) and (9) differ slightly from equation (4) of *Siegel*2014 because the mixed layer was consistently shallower than the EZ; hence, vertical mixing losses did not substantially impact our EZ budgets.

Although all four of these algorithms have been used to estimate the sinking flux of particles, it should be noted that the *Dunne* 2005 and *Laws* 2011 algorithms were actually designed to estimate the *ef*-ratio or total export production (including active transport by diel vertically migrating organisms and passive export of DOC). Sediment trap and ^{234}Th measurements should thus be expected to slightly underestimate the

predictions of *Dunne* 2005 and *Laws* 2011. *Stukel et al.* [2013a] estimated that active transport was 19% of sinking flux in the CCE study region, thus putting a lower-limit estimate on this bias.

2.5. Statistical Analyses

To quantitatively assess model-data fits we used the correlation coefficient (cor, which quantifies whether or not the model and data vary together; exact model-data fit would have cor = 1), the average error (AE, which quantifies whether the model has a general tendency to over or underestimate the measured values; exact model-data fit would have AE = 0), and the root mean squared error (RMSE, which quantifies the magnitude of the discrepancy between model and data) [see *Stow et al.*, 2009]. AE is particularly important for determining each algorithm's ability to accurately estimate the magnitude of flux in the study region (and thus may be a better indicator of potential accuracy in inter-regional comparisons), while cor reflects each algorithm's ability to capture intra-regional variability in flux.

The magnitude of the absolute value of model-data misfit was positively correlated with measured export flux (i.e., the residual was not homoscedastic). However, we did not log-transform the data to normalize the residual distribution, because we believe that an algorithm's ability to accurately estimate export during high flux events is particularly important for constraining the magnitude of the global BCP. Log-transformation would decrease the relative importance of misfits during high export periods relative to the (more commonly sampled) low flux periods. Thus using the un-transformed data penalizes algorithms (particularly when calculating AE) that substantially inflate or deflate export estimates during high flux events. Since our model-data residuals were not normally distributed, we used nonparametric bootstrapping techniques (sampling with replacement) with 10,000 iterations to assess the uncertainty in model statistics (AE, RMSE, cor.).

Throughout this manuscript all uncertainty estimates given are ± standard error unless otherwise stated.

3. Results and Discussion

3.1. In Situ Measurements

Despite the restricted spatial domain of this study, the water parcels sampled during our Lagrangian experiments spanned a large portion of the productivity gradient found in the global ocean. SSChl spanned a 41X range, with maximum and minimum values of 3.71 and 0.09 mg Chl *a* m^{-3}, respectively. Similarly, sea surface primary productivity (SSPP) measured by $H^{14}CO_3^-$ uptake spanned a 35-fold range (3.19–113 mg C m^{-3} d^{-1}). The variability in vertically integrated PP was slightly less due to increased PP at depth when SSPP was reduced (304–2333 mg C m^{-2} d^{-1}). SST varied from 12.2 to 28.1°C, though cycles were clustered in the 12.2–17.2°C (CCE) and 27.5–28.1°C (CRD) ranges.

Grazing rate measurements (protozoan and mesozooplankton) were only available for CCE-P0605, CCE-P0704, CCE-P0810 and CRD cruises. Vertically integrated phytoplankton specific losses to protozoan grazers ranged from 0.07 to 0.39 d^{-1}, while comparable losses to mesozooplankton showed higher variability of 0.01–0.84 d^{-1}. These grazing losses can be compared to specific phytoplankton growth rates (determined from the protozoan grazing dilution method) of 0.07–0.76 d^{-1}. When grazing is instead reported as bulk carbon grazed by zooplankton (calculated as grazing multiplied by the ratio of ^{14}CPP to dilution-derived specific growth rates), protozoan grazing rates range from 138 to 3440 mg C m^{-2} d^{-1} and mesozooplankton grazing rates range from 47 to 4036 mg C m^{-2} d^{-1}.

Sediment trap measurements at the shallowest deployment depth beneath the EZ (varying from 50 to 100 m depth, see supporting information Table S1) varied from 32 to 437 mg C m^{-2} d^{-1} with a mean of 158 mg C m^{-2} d^{-1}. ^{234}Th-based measurements varied from 32 to 294 mg C m^{-2} d^{-1} with a mean of 123 mg C m^{-2} d^{-1}. Normalization of export to the base of the euphotic zone using our computed remineralization constants (equation (1)) led to an average increase in export estimates of 19 ± 12% (mean ± st. dev.; median = 15%). When carbon export measurements from ^{234}Th and sediment traps were compared for the same experiments, they showed generally good agreement (Figure 2), with Type II linear regression (Pearson's Major Axis [*York*, 1966]) suggesting that ^{238}U-^{234}Th measurements underestimated carbon export relative to sediment traps (or conversely that sediment traps overestimated export relative to ^{238}U-^{234}Th) during periods of high flux.

3.2. Satellite Comparisons

We used our in situ plankton community and SST measurements to generate estimates of carbon export from each of the four satellite algorithms outlined above for comparison to contemporaneous sediment trap and

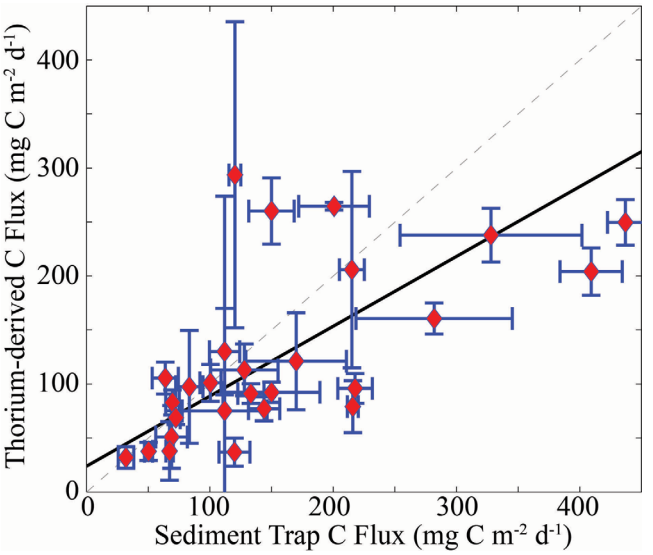

Figure 2. Comparison of sediment trap (x axis) and ^{238}U-^{234}Th-derived (y axis) organic carbon export at the shallowest trap depth (50–100 m). Solid line is the Type II linear regression (Th = 0.65×m + b, r^2=0.39, m=0.65 ± 0.16, b=24 ± 27). The dashed line is the 1:1 relationship. Error bars are one standard error of replicate measurements.

^{234}Th carbon export measurements (Figure 3). The two algorithms that estimate export efficiency using a combination of SST and either SSChl or PP (*Dunne*2005 and *Laws*2011) tended to overestimate export for our data set (Figures 3b, 3c, and 4; Table 2). When aggregating the sediment trap and ^{234}Th data, the AE for the *Laws*2011 model was +53 ± 21 mg C m^{-2} d^{-1}, while the AE for the *Dunne*2005 model was +82 ± 24 mg C m^{-2} d^{-1}. The third empirical model *Henson*2011, which uses SST alone to determine export efficiency was biased low (Figure 3d), with an AE (compared to export at 100 m depth horizon) of −47 ± 8 mg C m^{-2} d^{-1}. In terms of AE, the *Siegel*2014 algorithm performed best, with an AE of +20 ± 29 when calculated using size-fractionated Chl and +39 ± 12 mg C m^{-2} d^{-1} when calculated using microscopy (Mic) to determine the ratio of P_M:(P_M+P_S).

When compared based on RMSE, *Henson*2011 (evaluated at 100 m) clearly outperformed the other models, with an RMSE of 73 ± 8 mg C m^{-2} d^{-1}, although this is somewhat misleading because export at 100 m showed both lower values and lower variability (114 ± 61 for sediment trap and 109 ± 75 mg C m^{-2} d^{-1} for ^{234}Th, mean ± std) than at the base of the EZ (188 ± 133 for sediment trap and 146 ± 91 mg C m^{-2} d^{-1} for ^{234}Th). The other models performed fairly similarly with RMSE's of 125 ± 14, 162 ± 23, 185 ± 29, and 196 ± 28 mg C m^{-2} d^{-1} for *Siegel*2014 (Mic), *Laws*2011, *Siegel*2014 (Chl), and *Dunne*2005, respectively. Generally speaking, models showed little difference in their RMSE regardless of whether they were evaluated against sediment trap or ^{234}Th data, though there was (predictably) a constant offset in their AE, due to the 35 mg C m^{-2} d^{-1} difference between the means of the two measurements.

The *Siegel*2014 algorithm showed the greatest correlation with the data (Table 2), whether evaluated based on Chl (cor = 0.607 ± 0.149) or Mic (cor = 0.607 ± 0.088), although it was similar to the *Dunne*2005 algorithm (cor=0.606 ± 0.106). The *Laws*2011 and *Henson*2011 algorithms, by contrast, had lower correlation coefficients of 0.507 ± 0.112 and 0.521 ± 0.105, respectively. However, none of these differences in correlation were statistically significant.

To determine whether algorithms were systematically biased during high and/or low export periods, we binned the measurements into quartiles then calculated mean export measurement values and mean algorithm-derived export values (green diamonds in Figure 3). Results showed that *Laws*2011 was a slight overestimate for all quartiles, with a maximum overestimate of 60% in the third quartile. *Dunne*2005 also consistently overestimated flux, but was clearly more accurate at estimating flux during low export periods than during high export periods (when it overestimated flux by 90% and 38% for the third and fourth quartiles, respectively). *Henson*2011 underestimated flux in all quartiles, but by a substantially greater amount when export flux was high (50% underestimate in the fourth quartile). By contrast the *Siegel*2014 algorithm showed no strong difference between low and high export, with errors of 12%, −11%, 37%, and 17% for quartiles 1–4, respectively.

3.3. Food-Web and Export Flux Comparisons

A unique aspect of the explicit food web design of the *Siegel*2014 algorithm is the ability to predict grazing rates from satellite-derivable variables. Although G_M and G_S are explicitly formulated in the model as grazing on microphytoplankton and grazing on small phytoplankton, respectively, the implicit assumption is that G_M and G_S also represent the grazing rates of mesozooplankton and protozoans, respectively (hence

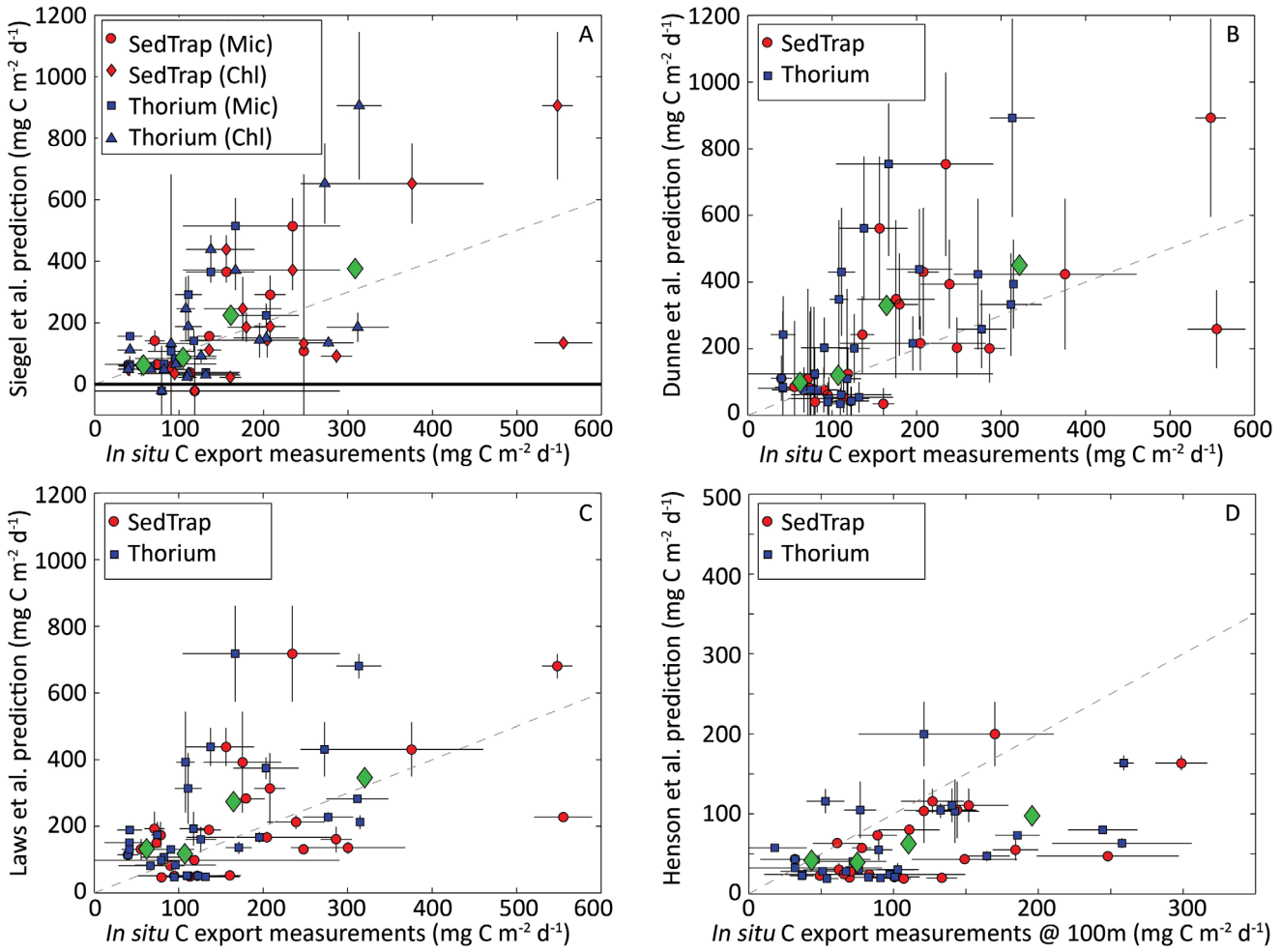

Figure 3. Comparison of satellite algorithms to in situ measurements. (a) Comparison of *Siegel*2014 algorithm to sediment trap (circles and diamonds) and ^{234}Th-derived (squares and triangles) measurements. Circles and squares are results using microscopy to determine the fraction of microphytoplankton. Diamonds and triangles are the results using size-fractionated Chl a to determine the fraction of microphytoplankton. (b, c, and d) The results of the *Dunne*2005, *Laws*2011, and *Henson*2011 models, respectively with circles showing sediment trap data and squares showing ^{234}Th data. All panels show export normalized to the base of the euphotic zone (EZ), except panel D, which shows export at 100 m. Green diamonds show arithmetic mean of predicted and measured export for each quartile of the measurements (35–85, 85–125, 125–205, and 205–560 mg C m^{-2} d^{-1} for base of EZ; 18–65, 65–89, 89–140, and 140–300 mg C m^{-2} d^{-1} for 100 m). Dashed lines depict a one-to-one relationship. Error bars show one standard error (for in situ measurements) and propagation of measurement standard error through satellite algorithms (for predictions).

FecM, the export efficiency of microphytoplankton is set to 0.3 [the typical egestion efficiency of mesozooplankton) [*Conover*, 1966] and FecS is set to 0.1 (close to the product of mesozooplankton egestion efficiency and typical protozoan gross growth efficiencies of 0.3 [*Straile*, 1997]). We can thus directly compare G_M and G_S to mesozooplankton and protozoan grazing rates measured by gut pigments and the protozoan grazing dilution method, respectively. Since our grazing measurements were based on Chl *a*, we converted to carbon units by multiplying specific grazing rates by the ratio of ^{14}CPP to specific growth rates determined by the dilution method (Figure 5). G_S showed a strikingly good comparison with protozoan grazing, except during two Lagrangian experiments: On Cycle 3 of CCE-P0605, in the midst of a dense bloom of large photosynthetic dinoflagellates, we measured very high protozoan grazing rates, but the *Siegel*2014 algorithm predicted low protozoan grazing rates (particularly when used with microscopy data that measured 89% of phytoplankton biomass to be >20 μm), shunting most of the production to mesozooplankton grazing and direct sinking of microphytoplankton cells. On Cycle 1 of CCE-P0810, we measured modest protozoan grazing rates, but the algorithm predicted negative grazing rates (for G_M and G_S) because measured net rates of change of vertically integrated Chl *a* in situ (0.24 d^{-1}) were only slightly less than measured specific growth rate (0.35 d^{-1}). Across the data set, protozoan grazing rates averaged 811 mg C m^{-2} d^{-1}, and the average error for G_S compared to protozoan grazing was -137 ± 117 mg C m^{-2} d^{-1}, with a correlation

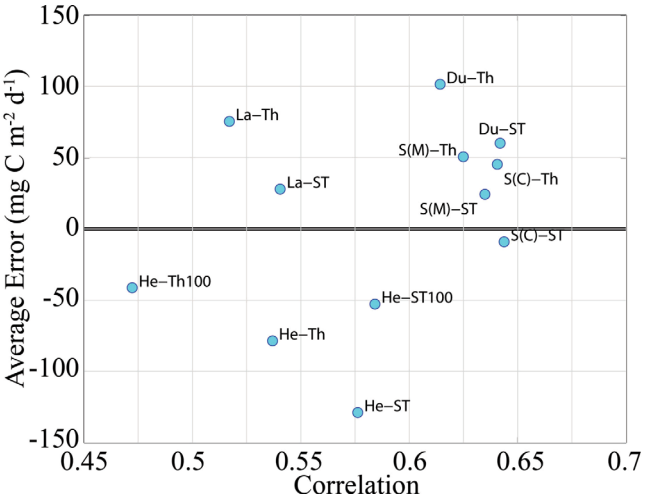

Figure 4. Model average error and correlation for different satellite algorithms when compared to ^{234}Th (Th) or sediment trap (ST) data. Models are *Laws*2011 (La), *Dunne*2005. (Du), *Henson*2011 (He), *Siegel*2011, with the fraction of microphytoplankton determined by microscopy (S(M)), and *Siegel*2011. with the fraction of microphytoplankton determined by size-fractionated Chl *a* (S(C)). All models are compared to export normalized to the depth of EZ except for He-Th100 and He-ST100, which were normalized to 100 m, since the *Henson*2011 algorithm was specifically designed for that depth.

of 0.58 ± 0.21 (p-value $= 6 \times 10^{-4}$). While measured protozoan grazing rates were well distributed across the data range from 0 to 1800 mg C m^{-2} d^{-1}, most of our mesozooplankton grazing rate measurements were $<$450 mg C m^{-2} d^{-1}, though the measurements showed a long tail with a maximum value of 4036 mg C m^{-2} d^{-1}. G_M consistently underestimated mesozooplankton grazing (21 out of 27 paired measurements). The measurement mean was 815 mg C m^{-2} d^{-1}, with an average error for G_M of -364 ± 121 mg C m^{-2} d^{-1}. G_M did, however, correlate well with measured mesozooplankton grazing, with a correlation coefficient of 0.76 ± 0.11 (p-value $= 4 \times 10^{-6}$). Taken together, these grazing comparisons support the use of the *Siegel*2014 algorithm.

The consistent negative bias of grazing rate estimates, however, does suggest a potential avenue for improving upon the *Siegel*2014 algorithm. G_M and G_S are calculated based on mass balance constraints between phytoplankton production, intrinsic nongrazing mortality, and net biomass accumulation (and also microphytoplankton sinking losses for G_M). Grazing is thus dependent on the parameters m_{Ph} (phytoplankton specific mortality) and f_{Alg} (the proportion of microphytoplankton production that is exported as sinking ungrazed cells). *Siegel*2014 took the reasonable approach of utilizing values for these parameters (0.1 d^{-1} for m_{Ph} and 0.1 for f_{Alg}) that are representative of similar values used in coupled biogeochemical models. However, despite their common use in models, these parameters are poorly constrained by in situ measurements. Nongrazer related mortality is a poorly understood process in the ocean, and is likely substantially less than grazing losses, with the potential exception of brief periods of high viral lysis [*Brum et al*., 2014]. Given the typical specific grazing rates measured in this study (median 0.17 d^{-1} for protozoans and 0.11 d^{-1} for mesozooplankton), the $m_{Ph} = 0.1$ d^{-1} value used by *Siegel*2014 would suggest that nongrazer related mortality is in fact closer to 25% of total mortality. It is thus reasonable to suggest that in the CCE and CRD m_{Ph} may be lower than assumed by *Siegel*2014. f_{Alg}, the fraction of phytoplankton production that is exported, is likely highly variable in the ocean and dependent on processes such as mineral ballasting [*Armstrong et al*., 2009], exopolymer production [*Passow*, 2002], and aggregation [*Alldredge and Silver*, 1988; *Guidi et al*., 2008]. Within the *Siegel*2014 algorithm, decreases in f_{Alg} lead to increases in G_M without commensurate increases in G_S.

Table 2. Summary Statistics (Average Error, Root Mean Squared Error, Correlation) for Model Comparisons to Measured Export (^{234}Th and Sediment Trap)[a]

Model	AE	RMSE	Cor
*Dunne*2005	$+82 \pm 24$	196 ± 28	0.61 ± 0.1
*Laws*2011	$+53 \pm 21$	162 ± 23	0.51 ± 0.11
*Henson*2011	-102 ± 13	140 ± 18	0.53 ± 0.1
*Henson*2011(100)	-47 ± 8	73 ± 8	0.52 ± 0.1
*Siegel*2014	$+28 \pm 20$	163 ± 21	0.61 ± 0.12
*Siegel*2014*	$+7 \pm 17$	135 ± 19	0.62 ± 0.13

[a]All model comparisons are to export measurements at the base of the euphotic zone except for *Henson*2011(100) which is to export at 100 m depth. *Siegel*2014* is with modified parameters (see *food web and flux comparisons* section), fAlg=0, mPh=0.037, γ determined in situ to be 0.0063 m^{-1} for CCE and 0.0024 m^{-1} for CRD. Uncertainties are $\pm$ standard error determined by bootstrapping.

We tested alternative versions of the *Siegel*2014 algorithm in which the parameters m_{Ph} and f_{Alg} were decreased to values of 0.05 or 0.0 (Figures 6a and 6b). Each set of parameters was evaluated based on its RMSE, average error, and correlation to the grazing data (with protozoan and mesozooplankton grazing results treated identically for this analysis). Decreasing f_{Alg} led to increased estimates of G_M, while decreasing

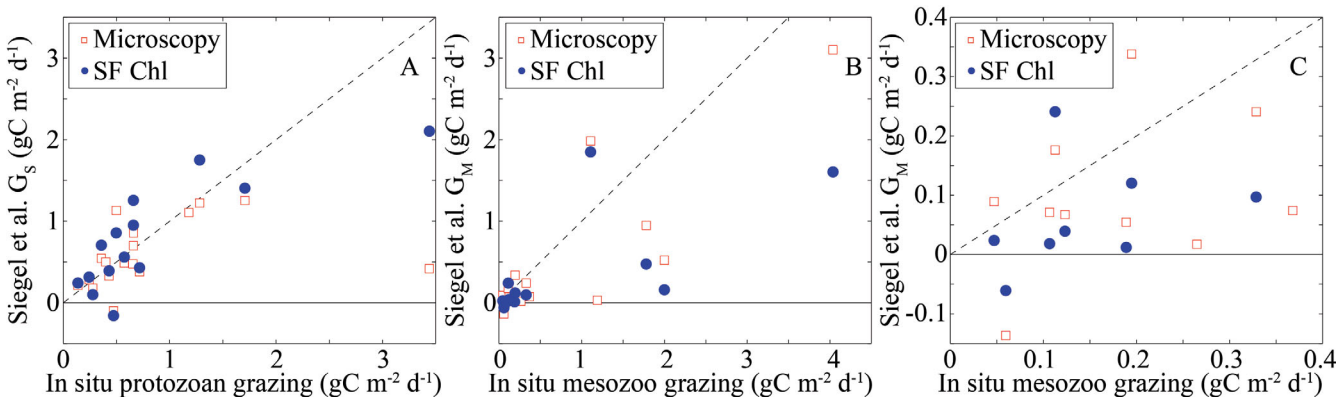

Figure 5. Comparison of in situ measured grazing rates (x axis) and *Siegel*2011 algorithm estimates (y axis). (a) Protozoan grazing measured by the dilution method (converted to carbon units by multiplying by the ratio of ^{14}CPP to phytoplankton specific growth rate determined by the dilution method) and *Siegel*2011 grazing on small (pico+nano) phytoplankton. (b) Mesozooplankton grazing measured by the gut pigment method (similarly converted to carbon units) and *Siegel*2011 grazing on microphytoplankton. (c) Same as Figure 5b, but with modified axes to highlight the many measurements of low grazing rates. In all plots open squares are for the *Siegel*2011 algorithm with microscopy used to determine the ratio of large phytoplankton to total phytoplankton biomass and closed circles are for the same algorithm when size-fractionated Chl *a* is used to determine that ratio. Dashed lines are 1:1 lines.

m_{Ph} led to increased estimates of both G_M and G_S. Since, both G_M and G_S underestimated the field-measured grazing rates of mesozooplankton and protozoans, respectively, decreasing both m_{Ph} and f_{Alg} decreased the absolute average errors of the models. When comparing the different simulations, four simulations that all had values of m_{Ph} and f_{Alg} between 0 and 0.05 (parameter sets 3–6 in Figures 6a and 6b) comprised a group that had the lowest RMSE and absolute average error. We also computed the parameter

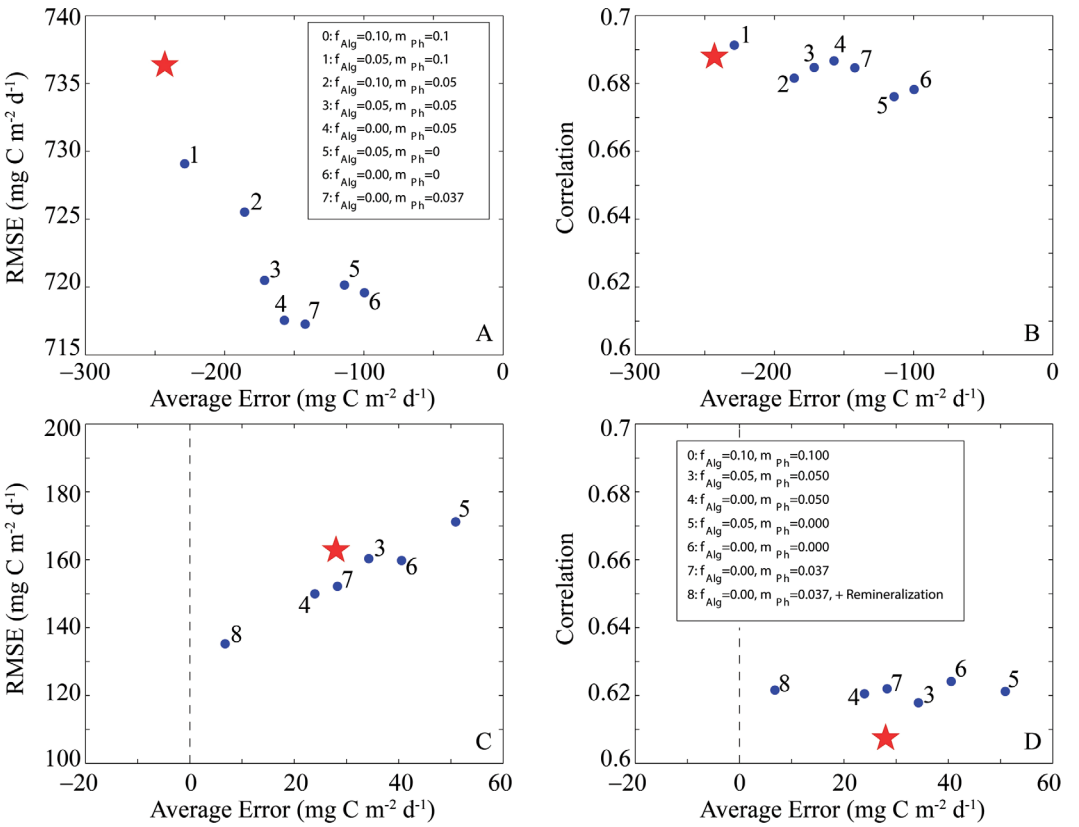

Figure 6. Root mean squared error (RMSE), average error, and correlation of in situ measurements of (a, b) grazing and (c, d) export to Siegel et al. algorithm with different parameter choices for f_{Alg} and m_{Ph}. In all figures, the star represents the parameterization in *Siegel*2011 (f_{Alg} = 0.1 and m_{Ph} = 1 d^{-1}). Parameterization 7 was empirically chosen to minimize the RMSE with respect to grazing. Parameterization 8 had the same f_{Alg} and m_{Ph} as 7, but with particle remineralization in the EZ.

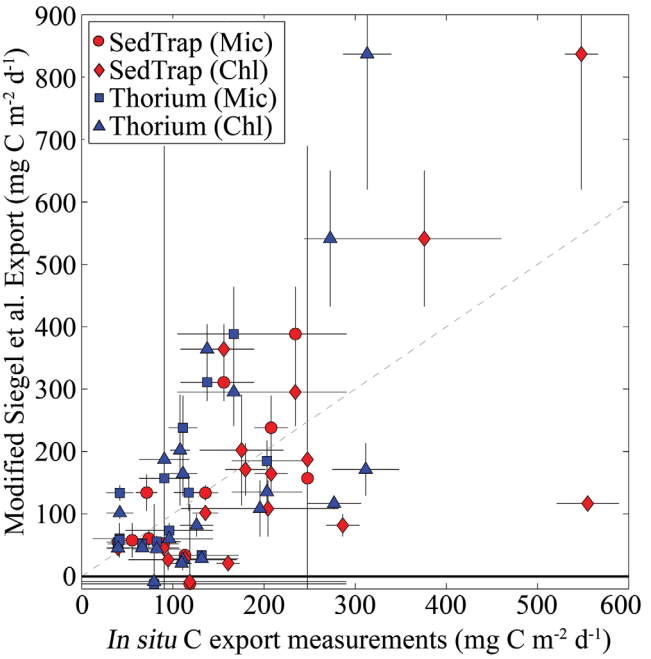

Figure 7. Comparison of in situ data to *Siegel*2011 algorithm with $f_{Alg} = 0$, $m_{Ph} = 0.037\ d^{-1}$, and a remineralization constant of $0.0063\ m^{-1}$ for CCE and $0.0024\ m^{-1}$ for CRD. The dashed line represents a 1:1 relationship.

combination that minimized the grazing RMSE ($f_{Alg} = 0$, $m_{Ph} = 0.037$, parameter set 7 on Figures 6a and 6b). We then computed a modified estimate of export from the *Siegel*2014 algorithm using these parameters (Figures 6c and 6d). Parameter sets 4 and 7 (the parameter sets with the lowest RMSE for grazing) performed particularly well with respect to export, leading to decreased RMSE and higher correlations with export measurements. Both, however, still had a similar average error relative to the initial *Siegel*2014 formulation, which (although better than the empirical algorithms) still overestimated export by 28 mg C m^{-2} d^{-1}.

It is important to note that when *Siegel*2014 parameterized the fraction of grazing on microphytoplankton exported as fecal material (f_{FecM}) as equal to typical egestion efficiencies of mesozooplankton (0.3) [*Conover*, 1966], they made the implicit assumption that all fecal pellets were exported out of the base of the EZ. This is only true if no fecal pellet remineralization occurs within the euphotic zone. While fecal pellets typically have high sinking velocities [*Turner*, 2015, and references therein], they can also be rapidly colonized by bacteria and protists [*Poulsen and Iversen*, 2008] and consumed or broken apart by mesozooplankton [*Paffenhöfer and Strickland*, 1970; *Lampitt et al*., 1990]. Thus, the estimate of fecal matter generation by the *Siegel*2014 algorithm likely overestimates the vertical flux of fecal matter reaching the base of the EZ. We therefore suggest that a remineralization rate be incorporated into the *Seigel*2014 model, such that equation (5) is modified to:

$$E_{EZ,Siegel,modified} = (AlgEZ + FecEZ) \times e^{-\gamma \times EZ/2} \quad (10)$$

where EZ/2 is half the depth of the euphotic zone (thus assuming that particles are generated evenly throughout the EZ) and γ is a remineralization constant. Here we use values of γ determined experimentally just beneath the euphotic zone by sediment traps deployed at multiple depths ($\gamma = 0.0063\ m^{-1}$ for CCE and $0.0024\ m^{-1}$ for CRD, see equation (1) in methods section). It is important to note that this is a parameter determined by measurements and not tuned to the data. However, it is likely to vary between ecosystems and may not be possible to estimate accurately from satellite products (though it may be correlated with temperature, particle concentration, or algorithm-derived G_M).

Using this minor modification to the *Siegel*2014 algorithm and the parameter set that minimized the RMSE with respect to grazing, the algorithm gives improved agreement between model and measured export values, with an average error of $+6.8 \pm 17$ mg C m^{-2} d^{-1}, an RMSE of 135 ± 19 mg C m^{-2} d^{-1}, and a correlation of 0.62 ± 0.13. With this parameterization, the model-data mismatch is within one standard error of zero for 41% of the measurements and within two standard errors for 62% of the measurements (Figure 7).

3.4. Ecosystem Considerations

The *Siegel*2014 parameters m_{Ph}, f_{Alg}, f_{FecM}, and f_{FecS} encode specific information about how ecosystems function. Given the diverse connections between plankton communities and biogeochemical cycles in marine ecosystems, these parameters may vary considerably in the ocean. Tuning the parameters of m_{Ph} and f_{Alg} so as to minimize the RMSE of model predictions with respect to protozoan and mesozooplankton

grazing rate measurements for data from the CCE and CRD suggested values that were significantly different from the best guess parameterizations of *Siegel*2014. While our parameters might not be a better fit for the global ocean, they do fit the CCE and CRD ecosystems (note that similar best fit parameters were found for each ecosystem CCE: $f_{Alg}=0.0$, $m_{Ph}=0.036$; CRD: $f_{Alg}=0.0$, $m_{Ph}=0.054$). These parameter values thus give insight into functional relationships for those systems.

For both CCE and CRD, the best fit to the in situ data was $f_{Alg}=0.0$, which suggests that intact microphytoplankton were not contributing significantly to export out of the euphotic zone. While ungrazed microphytoplankton are unquestionably a substantial contributor to export in some marine ecosystems, such as the subarctic North Atlantic [*Martin et al*., 2011], their negligible impact in the CCE and CRD is not surprising. Pigment analyses from sediment trap studies in both regions show very low concentrations of Chl *a*, with phaeopigment:Chl *a* ratios that were high enough to suggest that all of the Chl *a* found in the traps could have been transported undegraded within fecal pellets [*Stukel et al*., 2013a,b].

Specific nongrazer induced mortality rates, m_{Ph}, are difficult to assess for protistan communities, since cells can remain viable despite long periods of dormancy. However, parameters that are functionally similar to m_{Ph} are almost always utilized in NPZD-type biogeochemical and ecosystem models, where they function as closure terms that prevent population persistence at low concentration in suboptimal conditions (such as the deep sea) and return particulate matter to the dissolved phase. This term has been alternately interpreted as true mortality, as a specific respiration rate of the phytoplankton, or as a loss rate due to sinking, mixing or transport out of the EZ. It is usually tuned to maintain healthy populations in the surface layers, with little consideration to actual phytoplankton mortality sources in the ocean (such as programmed cell death or peroxide induced necrosis [*Brum et al*., 2014]). Our results suggest that m_{Ph} may be significantly lower than assumed by *Siegel*2014, at least in the CCE and CRD. The best estimate for m_{Ph} in our data set (0.037 d^{-1}), is at the low end of mortality values used in ecosystem models [e.g., *Fasham et al*., 1990; *Follows et al*., 2007; *Kishi et al*., 2007], suggesting that grazers may be responsible for a larger proportion of phytoplankton mortality than generally assumed in these model simulations.

3.5. Conclusions and Future Directions

This study was undertaken to assess the validity of underlying relationships for four algorithms that estimate the magnitude of the BCP from satellite measurements. It was not, however, an assessment of each algorithms' overall skill in predicting carbon export from remotely sensed products. Thus, our finding that the *Siegel*2014 algorithm returned results closest to the measured carbon export estimates from field experiments does not necessarily indicate that it is currently the best method for estimating export from space. The remote measurements required for the *Siegel*2014 algorithm, specifically the rate of change of SSChl and the phytoplankton size spectrum, are products with much greater uncertainties than the input requirements of other algorithms (such as SST). However, our results do demonstrate that the *Siegel*2014 algorithm is a useful foundation, with mechanistic linkages that should be further refined in future studies.

In that regard, substantial work needs to be done for model validation. Our results suggest that in the CCE and CRD the best fits to the data are obtained with lower values of f_{Alg} and m_{Ph} than suggested by *Siegel*2014 and that an EZ remineralization term should be included to account for remineralization between the depth of particle generation and the base of the EZ. All of these parameters (as well as f_{FecM} and f_{FecS}) likely respond to regional and temporal variability in the structure and dynamics of plankton communities, which should be a priority for understanding in future research. Lagrangian studies that simultaneously measure properties of the phytoplankton community (including in situ net rates of change) along with zooplankton grazing rates and carbon export are a powerful tool for answering these questions. We strongly recommend the use of such approaches in other regions in order to assess the variability of key parameters (f_{Alg}, m_{Ph}, f_{FecM}, f_{FecS}, and γ). While the difficulty and expense of these studies precludes the possibility of determining each parameter in every ecosystem and season, the robustness of remote-sensing measurements of export flux could be enhanced by experiments conducted over a range of ecosystem states to elucidate relationships between these parameters and satellite-observable properties.

Acknowledgments
The in situ data used for this manuscript can be found in the supporting information Table S1. Most of these data are derived from data freely available on the CCE LTER Datazoo repository (http://oceaninformatics.ucsd.edu/datazoo/data/ccelter/datasets) or the BCO-DMO website for CRD FLUZIE (http://www.bco-dmo.org/deployment/58834). This research was supported by NSF grants OCE-0417616 and OCE-1026607 for the CCE LTER site and OCE-0826626 (to MRL) for the CRD study. We are also indebted to the UC Ship Funds for providing funding for the NH0904 student-led cruise. This manuscript would not have been possible without the support of many friends and collaborators over the course of many months at sea. We would like to particularly thank Darcy Taniguchi, Karen Selph, Jesse Powell, Andrew Taylor, and Ally Pasulka. We would also like to thank the wonderful captain, crew, and research technicians of the R/V Melville, R/V Knorr, R/V Thompson, and R/V New Horizon who did an excellent job in facilitating our research goals.

References

Alldredge, A. L., and M. W. Silver (1988), Characteristics, dynamics and significance of marine snow, *Prog. Oceanogr.*, *20*(1), 41–82.
Armstrong, R. A., M. L. Peterson, C. Lee, and S. G. Wakeham (2009), Settling velocity spectra and the ballast ratio hypothesis, *Deep Sea Res., Part II*, *56*(18), 1470–1478, doi:10.1016/j.dsr2.2008.11.032.
Baker, E. T., H. B. Milburn, and D. A. Tennant (1988), Field assessment of sediment trap efficiency under varying flow conditions, *J. Mar. Res.*, *46*(3), 573–592.
Bednarsek, N., and M. D. Ohman (2015), Changes in pteropod distributions and shell dissolution across a frontal system in the California Current System, *Mar. Ecol. Prog. Ser.*, *523*, 93–103, doi:10.3354/meps11199.
Behrenfeld, M. J., and P. G. Falkowski (1997), Photosynthetic rates derived from satellite-based chlorophyll concentration, *Limnol. Oceanogr.*, *42*(1), 1–20.
Bishop, J. K. B. (2009), Autonomous observations of the ocean biological carbon pump, *Oceanography*, *22*(2), 182–193.
Boyd, P. W., and T. W. Trull (2007), Understanding the export of biogenic particles in oceanic waters: Is there consensus?, *Prog. Oceanogr.*, *72*(4), 276–312.
Brum, J. R., J. J. Morris, M. Décima, and M. R. Stukel (2014), Mortality in the oceans: Causes and consequences, in *Eco-DAS IX Symposium Proceedings*, edited by P. F. Kemp, pp. 16–48, Assoc. for the Sci. of Limnol. and Oceangr., Waco, Tex., doi:10.4319/ecodas.2014.978-0-9845591-3-8.16.
Brzezinski, M. A., J. W. Krause, R. M. Bundy, K. A. Barbeau, P. Franks, R. Goericke, M. R. Landry, and M. R. Stukel (2015), Enhanced silica ballasting from iron stress sustains carbon export in a frontal zone within the California Current, *J. Geophys. Res. Oceans*, *120*, 4654–4669, doi:10.1002/2015JC010829.
Buesseler, K. O., M. P. Bacon, J. K. Cochran, and H. D. Livingston (1992), Carbon and nitrogen export during the JGOFS North Atlantic Bloom Experiment estimated from ^{234}Th:^{238}U disequilibria, *Deep Sea Res., Part A*, *39*(7-8), 1115–1137.
Buesseler, K. O., et al. (2007), An assessment of the use of sediment traps for estimating upper ocean particle fluxes, *J. Mar. Res.*, *65*(3), 345–416.
Chen, J. H., R. L. Edwards, and G. J. Wasserburg (1986), ^{238}U, ^{234}U and ^{232}Th in seawater, *Earth Planet. Sci. Lett.*, *80*(3-4), 241–251.
Conover, R. J. (1966), Assimilation of organic matter by zooplankton, *Limnol. Oceanogr.*, *11*(3), 338–345.
Dam, H. G., and W. T. Peterson (1988), The effect of temperature on the gut clearance rate-constant of planktonic copepods, *J. Exp. Mar. Biol. Ecol.*, *123*(1), 1–14.
Décima, M., M. R. Landry, M. R. Stukel, L. Lopez-Lopez, and J. W. Krause (2015), Mesozooplankton biomass and grazing in the Costa Rica Dome: Amplifying variability through the plankton food web, *J. Plankton Res.*, doi:10.1093/plankt/fbv091, in press.
Ducklow, H. W., D. K. Steinberg, and K. O. Buesseler (2001), Upper ocean carbon export and the biological pump, *Oceanography*, *14*(4), 50–58.
Dunne, J. P., R. A. Armstrong, A. Gnanadesikan, and J. L. Sarmiento (2005), Empirical and mechanistic models for the particle export ratio, *Global Biogeochem. Cycles*, *19*, GB4026, doi:10.1029/2004GB002390.
Dunne, J. P., J. L. Sarmiento, and A. Gnanadesikan (2007), A synthesis of global particle export from the surface ocean and cycling through the ocean interior and on the seafloor, *Global Biogeochem. Cycles*, *21*, GB4006, doi:10.1029/2006GB002907.
Fasham, M. J. R., H. W. Ducklow, and S. M. McKelvie (1990), A nitrogen-based model of plankton dynamics in the oceanic mixed layer, *J. Mar. Res.*, *48*(3), 591–639.
Follows, M. J., S. Dutkiewicz, S. Grant, and S. W. Chisholm (2007), Emergent biogeography of microbial communities in a model ocean, *Science*, *315*(5820), 1843–1846, doi:10.1126/science.1138544.
Guidi, L., G. A. Jackson, L. Stemmann, J. C. Miquel, M. Picheral, and G. Gorsky (2008), Relationship between particle size distribution and flux in the mesopelagic zone, *Deep Sea Res., Part I*, *55*(10), 1364–1374, doi:10.1016/j.dsr.2008.05.014.
Henson, S. A., R. Sanders, E. Madsen, P. J. Morris, F. Le Moigne, and G. D. Quartly (2011), A reduced estimate of the strength of the ocean's biological carbon pump, *Geophys. Res. Lett.*, *38*, L04606, doi:10.1029/2011GL046735.
Henson, S. A., A. Yool, and R. Sanders (2015), Variability in efficiency of particulate organic carbon export: A model study, *Global Biogeochem. Cycles*, *29*, 33–45, doi:10.1002/2014GB004965.
Kishi, M. J., et al. (2007), NEMURO—A lower trophic level model for the North Pacific marine ecosystem, *Ecol. Modell.*, *202*(1-2), 12–25, doi:10.1016/j.ecolmodel.2006.08.021.
Knauer, G. A., J. H. Martin, and K. W. Bruland (1979), Fluxes of particulate carbon, nitrogen, and phosphorus in the upper water column of the Northeast Pacific, *Deep Sea Res., Part A*, *26*(1), 97–108.
Kostadinov, T. S., D. A. Siegel, and S. Maritorena (2009), Retrieval of the particle size distribution from satellite ocean color observations, *J. Geophys. Res.*, *114*, C09015, doi:10.1029/2009JC005303.
Kostadinov, T. S., D. A. Siegel, and S. Maritorena (2010), Global variability of phytoplankton functional types from space: Assessment via the particle size distribution, *Biogeosciences*, *7*(10), 3239–3257, doi:10.5194/bg-7-3239-2010.
Krause, J. W., M. A. Brzezinski, R. Goericke, M. R. Landry, M. D. Ohman, M. R. Stukel, and A. G. Taylor (2015), Variability in diatom contributions to biomass, organic matter production and export across a frontal gradient in the California Current Ecosystem, *J. Geophys. Res. Oceans*, *120*, 1032–1047, doi:10.1002/2014JC010472.
Lampitt, R. S., T. Noji, and B. von Bodungen (1990), What happens to zooplankton fecal pellets? Implications for material flux, *Mar. Biol.*, *104*(1), 15–23.
Landry, M. R., L. W. Haas, and V. L. Fagerness (1984), Dynamics of microbial plankton communities: Experiments in Kaneohe Bay, Hawaii, *Mar. Ecol. Prog. Ser.*, *16*(1-2), 127–133.
Landry, M. R., M. D. Ohman, R. Goericke, M. R. Stukel, and K. Tsyrklevich (2009), Lagrangian studies of phytoplankton growth and grazing relationships in a coastal upwelling ecosystem off Southern California, *Prog. Oceanogr.*, *83*, 208–216.
Landry, M. R., M. D. Ohman, R. Goericke, M. R. Stukel, K. A. Barbeau, R. Bundy, and M. Kahru (2012), Pelagic community responses to a deep-water front in the California Current Ecosystem: Overview of the A-Front Study, *J. Plankton Res.*, *34*(9), 739–748, doi:10.1093/plankt/fbs025.
Landry, M. R. A. de Verneil, J. I. Goes, and J. W. Moffett (in review), Plankton dynamics and biogeochemical fluxes in the Costa Rica Dome: Introduction to the CRD Flux and Zinc Experiments, *J. Plankton Res*. (submitted, 2015).
Laws, E. A. (2004), Export flux and stability as regulators of community composition in pelagic marine biological communities: Implications for regime shifts, *Prog. Oceanogr.*, *60*(2-4), 343–354.
Laws, E. A., P. G. Falkowski, W. O. Smith, H. Ducklow, and J. J. McCarthy (2000), Temperature effects on export production in the open ocean, *Global Biogeochem. Cycles*, *14*(4), 1231–1246.
Laws, E. A., E. D'Sa, and P. Naik (2011), Simple equations to estimate ratios of new or export production to total production from satellite-derived estimates of sea surface temperature and primary production, *Limnol. Oceanogr. Methods*, *9*, 593–601, doi:10.4319/lom.2011.9.593.

Martin, P., R. S. Lampitt, M. J. Perry, R. Sanders, C. Lee, and E. D'Asaro (2011), Export and mesopelagic particle flux during a North Atlantic spring diatom bloom, *Deep Sea Res., Part I*, *58*(4), 338–349, doi:10.1016/j.dsr.2011.01.006.

McDonnell, A. M. P., et al. (2015), The oceanographic toolbox for the collection of sinking and suspended marine particles, *Prog. Oceanogr.*, *133*, 17–31, doi:10.1016/j.pocean.2015.01.007.

Ohman, M. D., J. R. Powell, M. Picheral, and D. W. Jensen (2012), Mesozooplankton and particulate matter responses to a deep-water frontal system in the southern California Current System, *J. Plankton Res.*, *34*(9), 815–827, doi:10.1093/plankt/fbs028.

Owens, S. A., K. O. Buesseler, and K. W. W. Sims (2011), Re-evaluating the ^{238}U-salinity relationship in seawater: Implications for the ^{238}U-^{234}Th disequilibrium method, *Mar. Chem.*, *127*(1-4), 31–39, doi:10.1016/j.marchem.2011.07.005.

Paffenhöfer, G. A., and J. D. Strickland (1970), A note on feeding of *Calanus helgolandicus* on detritus, *Mar. Biol.*, *5*(2), 97–99.

Passow, U. (2002), Transparent exopolymer particles (TEP) in aquatic environments, *Prog. Oceanogr.*, *55*(3-4), 287–333.

Passow, U., and C. A. Carlson (2012), The biological pump in a high CO_2 world, *Mar. Ecol. Prog. Ser.*, *470*, 249–271, doi:10.3354/meps09985.

Pike, S. M., K. O. Buesseler, J. Andrews, and N. Savoye (2005), Quantification of ^{234}Th recovery in small volume sea water samples by inductively coupled plasma-mass spectrometry, *J. Radioanal. Nucl. Chem.*, *263*(2), 355–360.

Poulsen, L. K., and M. H. Iversen (2008), Degradation of copepod fecal pellets: Key role of protozooplankton, *Mar. Ecol. Prog. Ser.*, *367*, 1–13, doi:10.3354/meps07611.

Raven, J. A., and P. G. Falkowski (1999), Oceanic sinks for atmospheric CO2, *Plant Cell Environ.*, *22*(6), 741–755.

Savoye, N., C. Benitez-Nelson, A. B. Burd, J. K. Cochran, M. Charette, K. O. Buesseler, G. A. Jackson, M. Roy-Barman, S. Schmidt, and M. Elskens (2006), ^{234}Th sorption and export models in the water column: A review, *Mar. Chem.*, *100*(3-4), 234–249.

Selph, K. E., M. R. Landry, A. G. Taylor, A. Gutierrez-Rodriguez, M. R. Stukel, J. Wokuluk, and A. Pasulka (2015), Phytoplankton production and taxon-specific growth rates in the Costa Rica Dome, *J. Plankton Res.*, doi:10.1093/plankt/fbv063, in press.

Siegel, D. A., K. O. Buesseler, S. C. Doney, S. F. Sailley, M. J. Behrenfeld, and P. W. Boyd (2014), Global assessment of ocean carbon export by combining satellite obervations and food-web models, *Global Biogeochem. Cycles*, *28*, 181–196, doi:10.1002/2013GB004743.

Stow, C. A., J. Jolliff, D. J. McGillicuddy, S. C. Doney, J. I. Allen, M. A. M. Friedrichs, K. A. Rose, and P. Wallheadg (2009), Skill assessment for coupled biological/physical models of marine systems, *J. Mar. Syst.*, *76*(1–2), 4–15, doi:10.1016/j.jmarsys.2008.03.011.

Straile, D. (1997), Gross growth efficiencies of protozoan and metazoan zooplankton and their dependence on food concentration, predator-prey weight ratio, and taxonomic group, *Limnol. Oceanogr.*, *42*(6), 1375–1385.

Strickland, J. D., and T. R. Parsons (1972), *A Practical Handbook of Seawater Analysis*, *Bull. 167*, 2nd ed., Fish. Res. Board of Can., Ottawa.

Stukel, M. R., M. R. Landry, C. R. Benitez-Nelson, and R. Goericke (2011), Trophic cycling and carbon export relationships in the California Current Ecosystem, *Limnol. Oceanogr. Methods*, *56*(5), 1866–1878.

Stukel, M. R., M. R. Landry, M. D. Ohman, R. Goericke, T. Samo, and C. R. Benitez-Nelson (2012), Do inverse ecosystem models accurately reconstruct plankton trophic flows? Comparing two solution methods using field data from the California Current, *J. Mar. Syst.*, *91*(1), 20–33, doi:10.1016/j.jmarsys.2011.09.004.

Stukel, M. R., M. D. Ohman, C. R. Benitez-Nelson, and M. R. Landry (2013a), Contributions of mesozooplankton to vertical carbon export in a coastal upwelling system, *Mar. Ecol. Prog. Ser.*, *491*, 47–65, doi:10.3354/meps10453.

Stukel, M. R., M. Décima, K. E. Selph, D. A. A. Taniguchi, and M. R. Landry (2013b), The role of Synechococcus in vertical flux in the Costa Rica upwelling dome, *Prog. Oceanogr.*, *112-113*, 49–59, doi:10.1016/j.pocean.2013.04.003.

Stukel, M. R., C. Benitez-Nelson, M. Décima, A. G. Taylor, C. Buchwald, and M. R. Landry (2015), The biological pump in the Costa Rica Dome: An open ocean upwelling system with high new production and low export, *J. Plankton Res.*, doi:10.1093/plankt/fbv097, in press.

Taylor, A. G., R. Goericke, M. R. Landry, K. E. Selph, D. A. Wick, and M. J. Roadman (2012), Sharp gradients in phytoplankton community structure across a frontal zone in the California Current Ecosystem, *J. Plankton Res.*, *34*(9), 778–789, doi:10.1093/plankt/fbs036, in press.

Taylor, A. G., M. R. Landry, A. Freibott, K. E. Selph, and A. Gutierrez-Rodriguez (2015), Patterns of microbial community biomass, composition and HPLC diagnostic pigments in the Costa Rica upwelling dome, *J. Plankton Res.*, doi:10.1093/plankt/fbv086, in press.

Turner, J. T. (2015), Zooplankton fecal pellets, marine snow, phytodetritus and the ocean's biological pump, *Prog. Oceanogr.*, *130*, 205–248, doi:10.1016/j.pocean.2014.08.005.

Westberry, T., M. J. Behrenfeld, D. A. Siegel, and E. Boss (2008), Carbon-based primary productivity modeling with vertically resolved photoacclimation, *Global Biogeochem. Cycles*, *22*, GB2024, doi:10.1029/2007GB003078.

York, D. (1966), Least squares fitting *of a straight line, Can. J. Phys.*, *44*(5), 1079–1086, doi:10.1139/p66-090.

Zhang, X., H. G. Dam, J. R. White, and M. R. Roman (1995), Latitudinal variations in mesozooplankton grazing and metabolism in the central tropical Pacific during the US JGOFS EqPac Study, *Deep Sea Res., Part II*, *42*(2-3), 695–714.